

Published in final edited form as:

Wiley Interdiscip Rev Syst Biol Med. 2013 ; 5(3): 381–390. doi:10.1002/wsbm.1211.

Mechano-sensing and transduction by endothelial surface glycocalyx: composition, structure, and function

Bingmei M. Fu* and John M. Tarbell

Department of Biomedical Engineering, The City College of the City University of New York, New York, NY, USA

Abstract

The endothelial cells (ECs) lining every blood vessel wall are constantly exposed to the mechanical forces generated by blood flow. The EC responses to these hemodynamic forces play a critical role in the homeostasis of the circulatory system. To ensure proper EC mechano-sensing and transduction, there are a variety of mechano-sensors and transducers that have been identified on the EC surface, intra- and trans-EC membrane and within the EC cytoskeleton. Among them, the most recent candidate is the endothelial surface glycocalyx (ESG), which is a matrix-like thin layer covering the luminal surface of the EC. It consists of various proteoglycans, glycosaminoglycans, and plasma proteins, and is close to other prominent EC mechano-sensors and transducers. The ESG thickness was found to be in the order of 0.1–1 μm by different visualization techniques and in different types of vessels. Detailed analysis on the electron microscopy (EM) images of the microvascular ESG revealed a quasi-periodic substructure with the ESG fiber diameter of 10–12 and 20 nm spacing between adjacent fibers. Atomic force microscopy and optical tweezers were applied to investigate the mechanical properties of the ESG on the cultured EC monolayers and in solutions. Enzymatic degradation of specific ESG glycosaminoglycan components was used to directly elucidate the role of the ESG in EC mechano-sensing and transduction by measuring the shear-induced productions of nitric oxide and prostacyclin, two characteristic responses of the ECs to the flow. The unique location, composition, and structure of the ESG determine its role in EC mechano-sensing and transduction.

INTRODUCTION

In addition to forming a transport barrier between the blood and vessel wall, vascular endothelial cells (ECs) play important roles in regulating circulation functions. Besides biochemical stimuli, blood flow-induced (hemodynamic) mechanical stimuli, such as shear stress, pressure and circumferential stretch, modulate EC morphology and functions by activating mechano-sensors, signaling pathways, and gene and protein expressions.¹ EC responses to the hemodynamic forces (mechano-sensing and transduction) are critical to maintaining normal vascular functions.^{2,3} Failure in mechano-sensing and transduction contributes to serious vascular diseases including hypertension, atherosclerosis, aneurysms, and thrombosis, to name a few.⁴

The hemodynamic forces that ECs experience are described in Figure 1(a). The force (per unit surface area) perpendicular to the EC (the vessel wall) is the pressure due to the hydrodynamic force generated by the heart. The human circulatory system is 400,000 miles long, and the magnitude of blood pressure is not uniform in all the blood vessels in the human body. The blood pressure ranges from almost 0 to ~120 mmHg for a healthy adult human under resting conditions.⁵ Another type of force (per unit surface area) which is tangential to the EC surface is called shear or shear stress. The shear is due to the friction between the circulating blood and the vessel wall and ranges 10–40 dyn/cm² for arterial ECs and 1–6 dyn/cm² for venous ECs.⁶ The third force that acts along the circumference of the vessel wall is named circumferential stretch (or wall tension), also due to the blood pressure. Like the pressure and shear, the stretch varies in different types of vessels and under resting and exercising conditions.

The above hemodynamic forces vary spatially in different organs (10⁻¹ m length scale) and tissues (10⁻² m) due to vascular sizes and patterns (e.g., branches and turns), and temporally due to the pulsatile and oscillatory nature of the blood flow in large vessels. Even at the cellular level (10⁻⁴ m) there is a spatial distribution of these forces⁷ (Figure 1(b)). To sense and transmit the constantly varying hemo-dynamic forces from the EC surface to its cytoplasm and further into the nucleus, a variety of mechano-sensors and transducers (with size in the range from 10⁻⁹ to 10⁻⁶ m) are required. So far, at least 10 candidates have been identified as mechano-sensors and transducers, including cell adhesion proteins (e.g., VE-cadherin, PECAM-1),^{8,9} ion channels,^{10,11} tyrosine kinase receptors (e.g., vascular endothelial growth factor receptor 2),⁹ G-protein-coupled receptors and G-proteins,⁶ caveolae,¹² primary cilia,¹³ actin filaments,¹⁴ nesprins,¹⁵ integrins,¹⁶ and endothelial surface glycocalyx (ESG)¹⁷ (Figure 2). Because of its proteoglycan and glycosaminoglycan (GAG) composition and structure, the ESG may cover the entire surface of the EC as shown in Figure 2 (the yellow coat), and thus can interact with other EC sensors and transducers to play a role in sensing and transmitting hemodynamic forces.

COMPOSITION AND ORGANIZATION OF ESG

Molecular Composition

The roles of mechano-sensing and transduction of ESG are based on its molecular composition and organization, which are cartooned in Figure 3 (see review¹⁸). The transmembrane syndecans and the membrane-bound glypicans are the major protein core families of heparan sulfate proteoglycans found on the EC plasma membrane.¹⁹ The GAGs in the ESG are heparan sulfate (HS), chondroitin sulfate (CS), and hyaluronic acid (HA). Of the three, the most abundant is HS, accounting for 50–90% of the total GAGs, the rest being comprised of CS and HA.²⁰ Owing to structural analogy with heparin, HS and associated proteoglycans have been the most extensively studied, with attention recently shifting toward their ability to function as signal transduction molecules.^{19,21} The core proteins of proteoglycans support the covalent attachment of GAGs.

Syndecans-1, -2, -4 have three GAG attachment sites, close to their N-terminus and distal to the apical surface, which are modified primarily by HS. Syndecan-1 contains two additional sites for CS those are close to the membrane. The cytoplasmic tails of syndecans associate

with the cytoskeleton through linker molecules such as ezrin, tubulin, syntenin, syndesmos, dynamin, and α -actinin to distribute force throughout the cell. They also associate directly with proteins involved in signaling. Glypican-1 is the only glypican expressed on ECs. Its ectodomain is thought to form a compact globular tertiary structure. Closer to the membrane, its three to four GAG attachment sites are exclusively attached with HS. Glypican-1 is bound directly to the plasma membrane through a C-terminal glycosylphosphatidylinositol (GPI) anchor, which localizes this proteoglycan to lipid rafts, e.g., caveolae, which are involved in vesicular transport and cell signaling through signaling molecules, most notably endothelial-type nitric oxide synthase (eNOS).

Compared to CS and HS, HA is a much longer disaccharide polymer, which is synthesized on the cell surface and is not covalently attached to a core protein, but obtains its negative charge from carboxyl groups that provide it with exceptional hydration properties. HA weaves into the ESG through its interaction with surface HA receptors, such as the transmembrane glycoprotein CD44, which resides in caveolae, and CS chains of syndecans. Besides proteoglycans and GAGs, glycoproteins with short-branched oligosaccharides attached to their core are found on the EC surface. These oligosaccharides are capped by sialic acids (SA), the 9-carbon monosaccharides that contribute to the net negative charge of the ESG. Many important receptors on the cell surface, including mechano-sensors and transducers such as selectins and integrins, and members of the immunoglobulin superfamily, have oligosaccharides attached to them and are classified as glycoproteins. The plasma proteins (e.g., albumin, orosomucoid) trapped in the GAGs to further organize and extend the ESG layer.^{22,23}

Organization

It is widely believed that the negatively charged GAGs in the ESG capture circulating plasma protein and form an interconnected gel-like structure in an aqueous environment.^{24–26} The ESG would collapse when a GAG component is significantly reduced. However, most recent study by Zeng et al.²⁷ observed that specific enzymatic removal of HS or HA did not result in cleavage or collapse of any of the remaining components. Simultaneous removal of CS and HA by chondroitinase did not affect HS. Their results suggest that all GAGs and adsorbed proteins are well intermixed within the structure of the ESG, but the GAG components do not interact with one another.

THICKNESS AND ULTRASTRUCTURE OF ESG

Thickness

In addition to its biochemical composition, the thickness and ultrastructure of the ESG determine its function as a mechano-sensor and transducer. The first visualization of the ESG by electron microscopy (EM) used the cationic dye ruthenium red that binds to acidic mucopolysaccharides and generates electron density in the presence of osmium tetroxide.²⁸ Subsequent studies^{20,29} used gold colloids and immunoperoxidase labeling. Adamson and Clough²² then demonstrated using a large charged marker protein (unable to penetrate the ESG), cationized ferritin (molecular weight ~450 kDa), that in the absence of plasma proteins, the ESG would collapse, presumably because of elimination of intramolecular

interactions with plasma proteins, and that its undisturbed thickness was several times greater than the 20 nm observed with ruthenium red.^{22,28} All these methods may suffer from dehydration artifacts associated with aqueous fixatives that likely dissolve all but the protein cores of proteoglycans and collapse the inherently hydrated structures. A method developed to preserve water soluble structures using fluorocarbons as non-aqueous carriers of osmium tetroxide was applied to microvessels to obviate some of these limitations by Sims and Horne.³⁰ Further elaborations of the fluorocarbon-glutaraldehyde fixation methods by Rostgaard and Qvortrup³¹ revealed a filamentous brush-like surface coating on capillary walls, but a layer thickness of less than 50 nm, suggesting a cleavage of more superficial matrix structures. All the foregoing EM studies revealed an ESG with a thickness less than 100 nm. Recently, van den Berg et al.³² used a new approach to stabilize the anionic carbohydrate structures on the ESG by Alcian blue 8GX. They found that the ESG thickness was 0.2–0.5 μm on rat left ventricular myocardial capillaries.

A direct *in vivo* measurement of the ESG thickness with the dye-exclusion technique was developed by Vink and Duling.³³ Using a 70 kD FITC-dextran plasma tracer, which they showed was sterically excluded by the ESG, they were able to provide the first estimate of the *in vivo* thickness of the ESG in capillaries of hamster cremaster muscle to be ~0.4–0.5 μm . Most recently, the ESG thickness was also estimated as ~0.5 μm in rat mesenteric post-capillary venules by FITC-dextran labeling with intravital microscopy.³⁴ This estimate of the *in vivo* thickness of the ESG is four to five times greater than previous estimates derived from EM studies. This discrepancy was a catalyst for much of the work that has followed on the estimation of ESG thickness and its function as a barrier in cellular interactions as well as a mechano-sensor and transducer of ECs. Using high-resolution, near-wall, intravital fluorescent micro-particle image velocimetry (μ -PIV) to examine the velocity profile near the vessel wall in post-capillary venules of the mouse cremaster muscle, Long et al.³⁵ and Smith et al.³⁶ produced estimates of glycocalyx thickness of order 0.5 μm .

The poor spatial resolution of an intravital optical microscope limits the accurate measurement of the ESG thickness.³⁷ New imaging methods have thus been developed by employing laser scanning confocal microscopy and multi-photon microscopy, and fluorescently tagged antibodies to HS or HA binding protein, or wheat germ agglutinin to label major components of the ESG. Application of these new methods has revealed a much thicker ESG in large blood vessels: 4.3–4.5 μm in the mouse common carotid artery,³⁸ 2.2 μm in the mouse internal carotid artery,³⁹ and 2.5 μm in the external carotid artery.⁴⁰ Ebong et al.⁴¹ presented the first cryo-EM images of *in vitro* ESG that avoided the dehydration artifacts of conventional EM and observed structures greater than 5 μm in thickness. Most recently, using high-sensitivity and high-resolution confocal microscopy and *in situ/in vivo* single microvessel and *ex vivo* aorta immunostaining, Yen et al.⁴² revealed that the thickness of the ESG on rat mesenteric and mouse cremaster capillaries and post-capillary venules is 1–1.5 μm . Surprisingly, there was no detectable ESG in arterioles by using fluorescence labeled anti-HS. The ESG thickness is 2–2.5 μm on rat and mouse aorta. They also observed that the ESG is continuously and evenly distributed on the aorta wall but not on the microvessel wall if looking at a vessel segment of length ~100 μm .

Ultrastructure

The ultrastructural organization of the ESG and its relation to the cytoskeleton components (e.g., F-actin) of ECs was first investigated by Squire et al.⁴³ Using computed autocorrelation functions and Fourier transforms of EM images of frog mesenteric microvessels, they identified a quasi-periodic substructure in the ESG, which is a 3D fibrous meshwork (Figure 4) with characteristic spacing of ~20 nm. The fiber diameter was observed as 10–12 nm. They also showed that the fibrous elements may occur in clusters with a common intercluster spacing of ~100 nm and may be linked to the underlying actin cortical cytoskeleton. Figure 5 shows a modified sketch of this ultrastructural ESG model by Weinbaum et al.⁴⁴ which conceptually describes the arrangement of core proteins in the ESG and its anchorage to the underlying actin cortical cytoskeleton. The recent study by Arkill et al.⁴⁵ observed similar ESG structures in mammalian microvessels of choroid, renal tubules, glomerulus, and psoas muscle, and was confirmed by a 3D reconstruction using electron tomography.⁴⁶ The thickness of the ESG observed by their EM method is ~100 nm, similar to what was previously found on frog mesenteric microvessels.²² The approximately 100-nm-thick structure may form an inner core of the ESG which determines the filtration and molecular sieve function of the microvessel wall to water and solutes while a micron scale outer structure may generate a buffer region for the lubrication of RBC movement and a barrier for WBC adhesion to the ECs forming the vessel wall. But how this structure plays a role in mechano-sensing and transduction remains to be elucidated.

ESG AS A MECHANO-SENSOR AND MECHANO-TRANSDUCER

Mechanical Properties of ESG

To sense and transmit the blood flow-induced forces from the ESG surface to the EC cell body and nucleus, it is necessary for the ESG fibers (core proteins and attached GAGs in Figures 4 and 5) to have a structural integrity, which is characterized by the flexural rigidity, EI. Applying a linear elasto-hydrodynamic model, Weinbaum et al.⁴⁴ predicted that EI of the ESG fibers is 700 pN nm² by matching the time-dependent restoration of the ESG after being crushed by the passage of a WBC in a tightly fitting capillary.³³ Later, Han et al.⁴⁸ developed a more sophisticated nonlinear elasto-hydrodynamic model that uses large deformation theory for elastica and a modified Brinkman equation to describe the local relative motion of the fibers and the fluid. Their prediction for the EI of the ESG fibers is 490 pN nm², comparable to the result predicted by the earlier linear model.⁴⁴

Nijenhuis et al.⁴⁹ used optically trapped sub-micron probe particles to measure the viscoelastic properties of an *in vitro* ESG model, which consists of a 2.5 mg/ml bulk solution of hyaluronan (HA) and other components of the ESG, including CS, HS, aggrecan, albumin, and plasma. They found that CS and aggrecan, which directly interact with HA, modify the viscoelastic properties of the HA solution, while HS, plasma, and albumin have no effects. Applying atomic force microscopy (AFM) micro-indentation method, the elastic modulus of the ESG on bovine lung microvascular endothelial cell (BLMVEC) monolayer was measured as ~0.3 kPa after enzyme treatment for HS and HA.⁵⁰ By using an AFM nano-indentation method, a more recent study by Bai and Wang⁵¹ determined the Young's

modulus of the ESG on human umbilical vascular endothelial cell (HUVEC) monolayer to be 0.39 kPa.

Evidence of Mechano-Sensing and Transduction by ESG

The evidence that supports a major role for the ESG in mechano-transduction comes from experiments in which enzymes were used to selectively degrade specific components of the ESG, followed by a reassessment of function, or from the use of bathing solutions without plasma proteins where the ESG is compromised²² and structural organization examined in response to flow.^{52,53} One assessment for the ESG role in mechano-sensing and transduction is to measure the flow-induced production of nitric oxide (NO). Compared with the no flow condition, the application of steady flow with 20 dyn/cm² shear stress rapidly increased NO production from the baseline level in the *in vitro* experiments on (bovine aortic endothelial cells) BAECs.⁵⁴ Enzymatic treatment for HS,⁵⁴ HA, and SA, but not CS⁵⁵ completely blocked flow-induced NO production without affecting receptor-mediated NO production by bradykinin and histamine, suggesting that the ESG has a direct effect on the NO production machinery.⁵⁵ Similar results were shown in intact vessels. Enzymatic removal of SA abolished flow-dependent vasodilation in rabbit mesenteric arteries⁵⁶ and NO production in rabbit femoral arteries.⁵⁷ More recent study by Mochizuki et al.⁵⁸ also demonstrated that enzyme treatment for HA inhibited the flow-induced NO production.

Surprisingly, Pahakis et al.⁵⁵ showed that none of the above four ESG-degrading enzymes had an inhibitory effect on flow-induced prostacyclin (PGI₂) production, another characteristic response of ECs to the flow,⁵⁹ suggesting that there are multiple mechanisms of mechano-transduction as well as multiple mechano-transducers facilitated by the EC to generate diverse biological responses.

Mechanisms of Mechano-Sensing and Transduction by ESG

When there is an intact ESG, the fluid flow in the ESG region is governed by a Brinkman equation including both effects of the ESG fibers and fluid viscosity, which is different from the Navier-Stokes equation, governing the viscous flow in the core region of the vessel. For this reason, the force acting on the EC membrane is no longer the shear, which is nearly zero at the bottom of the ESG. Instead, the EC cytoskeleton experiences a torque coming from the flow-induced drag force acting on the ESG fibers.^{44,60} There should be cytoskeleton components (e.g., actin filaments) and/or plasma membrane components that can transmit this torque into the cytoplasm and nucleus of ECs. However, when the ESG is degraded in diseases^{32,61} or the vessel segment is not significantly covered with the ESG,⁴² the flow-induced shear can directly act on the EC plasma membrane and cytoskeleton. Then other EC mechano-sensors and transducers come into play as summarized in the study by Yamamoto⁶ and demonstrated in Figure 2.

Two endothelial mechano-transduction mechanisms were proposed by Davies.⁶² One is decentralized mechanism in which mechano-sensing is at the EC surface while mechano-transduction occurs at sites distinct from the surface. Another is the centralized mechanism in which both sensing and transduction take place at the EC surface. The ESG mechano-transduction can progress through both mechanisms (Figure 3). In terms of the decentralized

mechanism, syndecans containing both HS and CS have an established association with the cytoskeleton,²¹ and through it can decentralize the signal by distributing it to multiple sites within the cell (i.e., nucleus, organelles, focal adhesions, intercellular junctions). For centralized sensing and transduction, glypicans containing HS, but not CS, are linked to caveolae where eNOS resides along with many other signaling molecules.¹⁸ The observation that depletion of HS, but not CS, inhibits shear-induced NO production, favors a glypican-caveolae-eNOS centralized mechanism. In addition, HA binds to its CD44 receptor that is localized in caveolae.^{63,64} This provides a link between HA and flow-induced NO. The role of SA in NO production is less clear, but it is known that CD44 can have oligosaccharides (that are capped by SA) attached to it.⁶³ The negative charge carried by the ESG components enhances hydration and extension of the multicomponent structure in aqueous media. Loss of charge through enzyme degradation could lead to partial collapse of the integrated structure and reduction of fluid shear sensing.⁵² The lack of influence of enzyme for CS may be associated with its location that is closer to the plasma membrane than the other components, thus allowing the more apical drag sensing elements to remain extended in its absence.

CONCLUSION

While the ESG has been studied for almost half-century in terms of its composition, structure and function, its role in EC mechano-sensing and transduction has just begun to be investigated. Owing to its heterogeneous structures, complex composition of various proteoglycans, GAGs, and adsorbed plasma proteins and attachment to the transmembrane glycoproteins and receptors, as well as EC cytoskeleton and plasma membrane, its function in sensing and transmitting hemodynamic forces is expected to be governed by multiple mechanisms and nonlinearly coupled with other well-known mechano-sensors and transducers including G-protein-coupled receptors, ion channels, tyrosine kinase receptors, cell adhesion molecules, caveolae, actin filaments, integrins, etc.

In future studies, along with the more advanced visualization and image processing techniques, the nano-micron structures of the ESG and their relations with other EC mechano-sensors and transducers will be detailed in all types of blood vessels and under physiological and pathological conditions. The mechanical properties of the ESG will be further investigated *in vivo* and *in vitro* using a variety of techniques such as atomic force microscopy, optical tweezers, and optic-acoustic techniques. Multi-scale mathematical models will be developed to decipher the role of the ESG in EC mechano-sensing and transduction on the basis of experimental results and observations. To completely elucidate the composition, structure, and function of the ESG, collaboration among multi-disciplines including biochemistry, molecular biology, physiology, physics, mathematics, and engineering is highly desired.

Acknowledgments

This work was supported by NIH/NHLBI 1R01HL094889. We thank Ms. Wanyi Yen for her help in finding some of the literature.

References

1. Mammoto A, Mammoto T, Ingber DE. Mechanosensitive mechanisms in transcriptional regulation. *J Cell Sci*. 2012; 125(Pt 13):3061–3073. [PubMed: 22797927]
2. Davies PF, Dewey CF Jr, Bussolari SR, Gordon EJ, Gimbrone MA Jr. Influence of hemodynamic forces on vascular endothelial function. In vitro studies of shear stress and pinocytosis in bovine aortic cells. *J Clin Invest*. 1984; 73:1121–1129. [PubMed: 6707208]
3. Chien S. Mechanotransduction and endothelial cell homeostasis: the wisdom of the cell. *Am J Physiol Heart Circ Physiol*. 2007; 292:H1209–H224. [PubMed: 17098825]
4. Ingber DE. Mechanobiology and diseases of mechanotransduction. *Ann Med*. 2003; 35:564–577. [PubMed: 14708967]
5. Fung, YC. *Biomechanics: Circulation*. New York: Springer; 1997. p. 571
6. Yamamoto K, Ando J. New molecular mechanisms for cardiovascular disease: blood flow sensing mechanism in vascular endothelial cells. *J Pharmacol Sci*. 2011; 116:323–331. [PubMed: 21757846]
7. Muller S, Labrador V, Da Isla N, Dumas D, Suna R, Wang X, Wei L, Fawzi-Grancher S, Yang W, Traore M, et al. From hemorheology to vascular mechanobiology: an overview. *Clin Hemorheol Microcirc*. 2004; 30:185–200. [PubMed: 15258343]
8. Stevens HY, Melchior B, Bell KS, Yun S, Yeh JC, Frangos JA. PECAM-1 is a critical mediator of atherosclerosis. *Dis Model Mech*. 2008; 1:175–181. [PubMed: 19048083]
9. Schwartz MA, DeSimone DW. Cell adhesion receptors in mechanotransduction. *Curr Opin Cell Biol*. 2008; 20:551–556. [PubMed: 18583124]
10. Gojova A, Barakat AI. Vascular endothelial wound closure under shear stress: role of membrane fluidity and flow-sensitive ion channels. *J Appl Physiol*. 2005; 98:2355–2362. [PubMed: 15705727]
11. Gautam M, Shen Y, Thirkill TL, Douglas GC, Barakat AI. Flow-activated chloride channels in vascular endothelium. Shear stress sensitivity, desensitization dynamics, and physiological implications. *J Biol Chem*. 2006; 281:36492–36500. [PubMed: 16973617]
12. Tabouillot T, Muddana HS, Butler PJ. Endothelial cell membrane sensitivity to shear stress is lipid domain dependent. *Cell Mol Bioeng*. 2011; 4:169–181. [PubMed: 22247740]
13. Egorova AD, van der Heiden K, Poelmann RE, Hierck BP. Primary cilia as biomechanical sensors in regulating endothelial function. *Differentiation*. 2012; 83:S56–S61. [PubMed: 22169885]
14. Matsui TS, Kaunas R, Kanzaki M, Sato M, Deguchi S. Non-muscle myosin II induces disassembly of actin stress fibres independently of myosin light chain dephosphorylation. *Interface Focus*. 2011; 1:754–766. [PubMed: 23050080]
15. Morgan JT, Pfeiffer ER, Thirkill TL, Kumar P, Peng G, Fridolfsson HN, Douglas GC, Starr DA, Barakat AI. Nesprin-3 regulates endothelial cell morphology, perinuclear cytoskeletal architecture, and flow-induced polarization. *Mol Biol Cell*. 2011; 22:4324–4334. [PubMed: 21937718]
16. Wang N, Tytell JD, Ingber DE. Mechanotransduction at a distance: mechanically coupling the extracellular matrix with the nucleus. *Nat Rev Mol Cell Biol*. 2009; 10:75–82. [PubMed: 19197334]
17. Tarbell JM, Ebong EE. The endothelial glycocalyx: a mechano-sensor and -transducer. *Sci Signal*. 2008; 1:pt8.10.1126/scisignal.140pt8 [PubMed: 18840877]
18. Tarbell JM, Pahakis MY. Mechanotransduction and the glycocalyx. *J Intern Med*. 2006; 259:339–350. [PubMed: 16594902]
19. Rosenberg RD, Shworak NW, Liu J, Schwartz JJ, Zhang L. Heparan sulfate proteoglycans of the cardiovascular system. Specific structures emerge but how is synthesis regulated? *J Clin Invest*. 1997; 100(11 Suppl):S67–S75. [PubMed: 9413405]
20. Sarrazin S, Lamanna WC, Esko JD. Heparan sulfate proteoglycans. *Cold Spring Harb Perspect Biol*. 2011; 3:a004952.10.1101/cshperspect.a004952 [PubMed: 21690215]
21. Tkachenko E, Rhodes JM, Simons M. Syndecans: new kids on the signaling block. *Circ Res*. 2005; 96:488–500. [PubMed: 15774861]

22. Adamson RH, Clough G. Plasma proteins modify the endothelial cell glycocalyx of frog mesenteric microvessels. *J Physiol.* 1992; 445:473–486. [PubMed: 1501143]
23. Friden V, Oveland E, Tenstad O, Ebefors K, Nystrom J, Nilsson UA, Haraldsson B. The glomerular endothelial cell coat is essential for glomerular filtration. *Kidney Int.* 2011; 79:1322–1330. [PubMed: 21412215]
24. Weinbaum S, Tarbell JM, Damiano ER. The structure and function of the endothelial glycocalyx layer. *Annu Rev Biomed Eng.* 2007; 9:121–167. [PubMed: 17373886]
25. Sorensson J, Ohlson M, Haraldsson B. A quantitative analysis of the glomerular charge barrier in the rat. *Am J Physiol Renal Physiol.* 2001; 280:F646–F656. [PubMed: 11249856]
26. Ohlson M, Sorensson J, Haraldsson B. A gel-membrane model of glomerular charge and size selectivity in series. *Am J Physiol Renal Physiol.* 2001; 280:F396–F405. [PubMed: 11181401]
27. Zeng Y, Ebong EE, Fu BM, Tarbell JM. The structural stability of the endothelial glycocalyx after enzymatic removal of glycosaminoglycans. *PLoS One.* 2012; 7:e43168.10.1371/journal.pone.0043168 [PubMed: 22905223]
28. Luft JH. Fine structures of capillary and endocapillary layer as revealed by ruthenium red. *Fed proc.* 1966; 25:1773–1783. [PubMed: 5927412]
29. Baldwin AL, Winlove CP. Effects of perfusate composition on binding of ruthenium red and gold colloid to glycocalyx of rabbit aortic endothelium. *J Histochem Cytochem.* 1984; 32:259–266. [PubMed: 6198357]
30. Sims DE, Horne MM. Non-aqueous fixative preserves macromolecules on the endothelial cell surface: an in situ study. *Eur J Morphol.* 1993; 31:251–255. [PubMed: 8172755]
31. Rostgaard J, Qvortrup K. Electron microscopic demonstrations of filamentous molecular sieve plugs in capillary fenestrae. *Microvasc Res.* 1997; 53:1–13. [PubMed: 9056471]
32. van den Berg BM, Vink H, Spaan JA. The endothelial glycocalyx protects against myocardial edema. *Circ Res.* 2003; 92:592–594. [PubMed: 12637366]
33. Vink H, Duling BR. Identification of distinct luminal domains for macromolecules, erythrocytes, and leukocytes within mammalian capillaries. *Circ Res.* 1996; 79:581–589. [PubMed: 8781491]
34. Gao L, Lipowsky HH. Composition of the endothelial glycocalyx and its relation to its thickness and diffusion of small solutes. *Microvasc Res.* 2010; 80:394–401. [PubMed: 20600162]
35. Long DS, Smith ML, Pries AR, Ley K, Damiano ER. Microviscometry reveals reduced blood viscosity and altered shear rate and shear stress profiles in microvessels after hemodilution. *Proc Natl Acad Sci U S A.* 2004; 101:10060–10065. [PubMed: 15220478]
36. Smith ML, Long DS, Damiano ER, Ley K. Near-wall micro-PIV reveals a hydrodynamically relevant endothelial surface layer in venules in vivo. *Biophys J.* 2003; 85:637–645. [PubMed: 12829517]
37. Pries AR, Secomb TW, Gaehtgens P. The endothelial surface layer. *Pflugers Arch.* 2000; 440:653–666. [PubMed: 11007304]
38. Megens RT, Reitsma S, Schiffers PH, Hilgers RH, De Mey JG, Slaaf DW, oude Egbrink MG, van Zandvoort MA. Two-photon microscopy of vital murine elastic and muscular arteries. Combined structural and functional imaging with subcellular resolution. *J Vasc Res.* 2007; 44:87–98. [PubMed: 17192719]
39. van den Berg BM, Spaan JA, Vink H. Impaired glycocalyx barrier properties contribute to enhanced intimal low-density lipoprotein accumulation at the carotid artery bifurcation in mice. *Pflugers Arch.* 2009; 457:1199–1206. [PubMed: 18839207]
40. Reitsma S, Oude Egbrink MG, Vink H, van den Berg BM, Lima Passos V, Engels W, Slaaf DW, van Zandvoort MA. Endothelial glycocalyx structure in the intact carotid artery: a two-photon laser scanning microscopy study. *J Vasc Res.* 2011; 48:297–306. [PubMed: 21273784]
41. Ebong EE, Macaluso FP, Spray DC, Tarbell JM. Imaging the endothelial glycocalyx in vitro by rapid freezing/freeze substitution transmission electron microscopy. *Arterioscler Thromb Vasc Biol.* 2011; 31:1908–1915. (Editorial: An 11- μ m-Thick Glycocalyx? It's All in the Technique! *Arterioscler Thromb Vasc Biol.* 31(8): 1712–1713, 2011). [PubMed: 21474821]
42. Yen WY, Cai B, Zeng M, Tarbell JM, Fu BM. Quantification of the endothelial surface glycocalyx on rat and mouse blood vessels. *Microvasc Res.* 2012; 83:337–346. [PubMed: 22349291]

43. Squire JM, Chew M, Nneji G, Neal C, Barry J, Michel C. Quasi-periodic substructure in the microvessel endothelial glycocalyx: a possible explanation for molecular filtering? *J Struct Biol.* 2001; 136:239–255. [PubMed: 12051903]
44. Weinbaum S, Zhang X, Han Y, Vink H, Cowin SC. Mechanotransduction and flow across the endothelial glycocalyx. *Proc Natl Acad Sci U S A.* 2003; 100:7988–7995. [PubMed: 12810946]
45. Arkill KP, Knupp C, Michel CC, Neal CR, Qvortrup K, Rostgaard J, Squire JM. Similar endothelial glycocalyx structures in microvessels from a range of mammalian tissues: evidence for a common filtering mechanism? *Biophys J.* 2011; 101:1046–1056. [PubMed: 21889441]
46. Arkill KP, Neal CR, Mantell JM, Michel CC, Qvortrup K, Rostgaard J, Bates DO, Knupp C, Squire JM. 3D reconstruction of the glycocalyx structure in mammalian capillaries using electron tomography. *Microcirculation.* 2012; 19:343–351. [PubMed: 22324320]
47. Clough G, Michel CC, Phillips ME. Inflammatory changes in permeability and ultrastructure of single vessels in the frog mesenteric circulation. *J Physiol.* 1988; 395:99–114. [PubMed: 3261792]
48. Han Y, Weinbaum S, Spaan JAE, Vink H. Large deformation analysis of the elastic recoil of fiber layers in a Brinkman medium with application to the endothelial glycocalyx. *J Fluid Mech.* 2006; 554:217–235.
49. Nijenhuis N, Mizuno D, Spaan JA, Schmidt CF. Viscoelastic response of a model endothelial glycocalyx. *Phys Biol.* 2009; 6:025014. [PubMed: 19571362]
50. O’Callaghan R, Job KM, Dull RO, Hlady V. Stiffness and heterogeneity of the pulmonary endothelial glycocalyx measured by atomic force microscopy. *Am J Physiol Lung Cell Mol Physiol.* 2011; 301:L353–L360. [PubMed: 21705487]
51. Bai K, Wang W. Spatio-temporal development of the endothelial glycocalyx layer and its mechanical property in vitro. *J R Soc Interface.* 2012; 9:2290–2298. [PubMed: 22417911]
52. Thi MM, Tarbell JM, Weinbaum S, Spray DC. The role of the glycocalyx in reorganization of the actin cytoskeleton under fluid shear stress: a “bumpercar” model. *Proc Natl Acad Sci.* 2004; 101:16483–16488. [PubMed: 15545600]
53. Yao Y, Rabodzey A, Dewey CF Jr. Glycocalyx modulates the motility and proliferative response of vascular endothelium to fluid shear stress. *Am J Physiol Heart Circ Physiol.* 2007; 293:H1023–H1030. [PubMed: 17468337]
54. Florian JA, Kosky JR, Ainslie K, Pang Z, Dull RO, Tarbell JM. Heparan sulphate proteoglycan is a mechanosensor on endothelial cells. *Circ Res.* 2003; 93:e136–e142. [PubMed: 14563712]
55. Pahakis MY, Kosky JR, Dull RO, Tarbell JM. The role of endothelial glycocalyx components in mechanotransduction of fluid shear stress. *Biochem Biophys Res Commun.* 2007; 355:228–233. [PubMed: 17291452]
56. Pohl U, Herlan K, Huang A, Bassenge E. EDRF-mediated shear-induced dilation opposes myogenic vasoconstriction in small rabbit arteries. *Am J Physiol.* 1991; 261:H2016–H2023. [PubMed: 1721502]
57. Hecker M, Mulsch A, Bassenge E, Busse R. Vasoconstriction and increased flow: two principal mechanisms of shear stress-dependent endothelial autacoid release. *Am J Physiol.* 1993; 265:H828–H833. [PubMed: 8105699]
58. Mochizuki S, Vink H, Hiramatsu O, Kajita T, Shigeto F, Spaan JA, Kajiya F. Role of hyaluronic acid glycosaminoglycans in shear-induced endothelium-derived nitric oxide release. *Am J Physiol.* 2003; 285:H722–H726.
59. Frangos JA, Eskin SG, McIntire LV, Ives CL. Flow effects on prostacyclin production by cultured human endothelial cells. *Science.* 1985; 227:1477–1479. [PubMed: 3883488]
60. Secomb TW, Hsu R, Pries AR. Effect of endothelial surface layer on transmission of fluid shear stress to endothelial cells. *Biorheology.* 2001; 38:143–150. [PubMed: 11381171]
61. Cai B, Fan J, Zeng M, Zhang L, Fu BM. Adhesion of malignant mammary tumor cells MDA-MB-231 to microvessel wall increases microvascular permeability via degradation of endothelial surface glycocalyx. *J Appl Physiol.* 2012; 113:1141–1153. [PubMed: 22858626]
62. Davies PF. Flow-mediated endothelial mechanotransduction. *Physiol Rev.* 1995; 75:519–560. [PubMed: 7624393]

63. Forster-Horvath C, Meszaros L, Raso E, Dome B, Ladanyi A, Morini M, Albini A, Timar J. Expression of CD44v3 protein in human endothelial cells in vitro and in tumoral microvessels in vivo. *Microvasc Res.* 2004; 68:110–118. [PubMed: 15313120]
64. Singleton PA, Bourguignon LY. CD44 interaction with ankyrin and IP3 receptor in lipid rafts promotes hyaluronan-mediated Ca²⁺ signaling leading to nitric oxide production and endothelial cell adhesion and proliferation. *Exp Cell Res.* 2004; 295:102–118. [PubMed: 15051494]

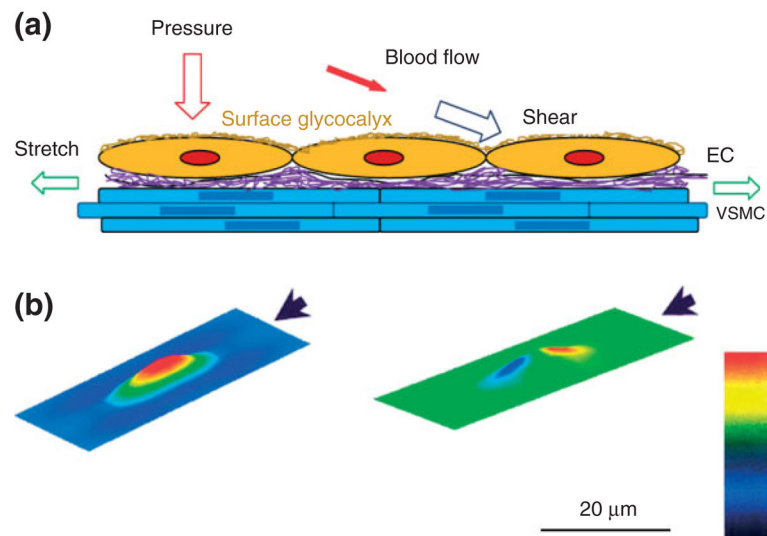


FIGURE 1.

(a) Schematic for the forces acting on endothelial cells (ECs) forming the blood vessel wall. Pressure (perpendicular to the ECs) and stretch (in line of the circumferential direction of the vessel wall) due to the blood pressure, shear (tangential to the ECs) due to the blood flow and blood viscosity. Vascular smooth muscle cell (VSMC); purple represents the extra cellular matrix (ECM); at the luminal surface of ECs, there is a thin layer of surface glycocalyx. (b) Predictions from a theoretical model for the distribution of the shear stress (left) and that of the pressure (right) on the surface of the EC. The direction of the flow is represented by the arrow. The bar indicates the magnitude from low (black) to high (red). (Figure 1(b): Reprinted with permission from Ref 7. Copyright 2004 IOS press)

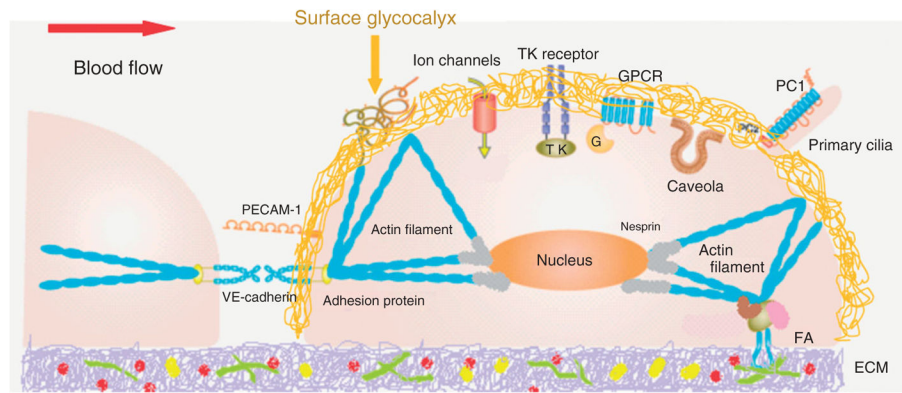
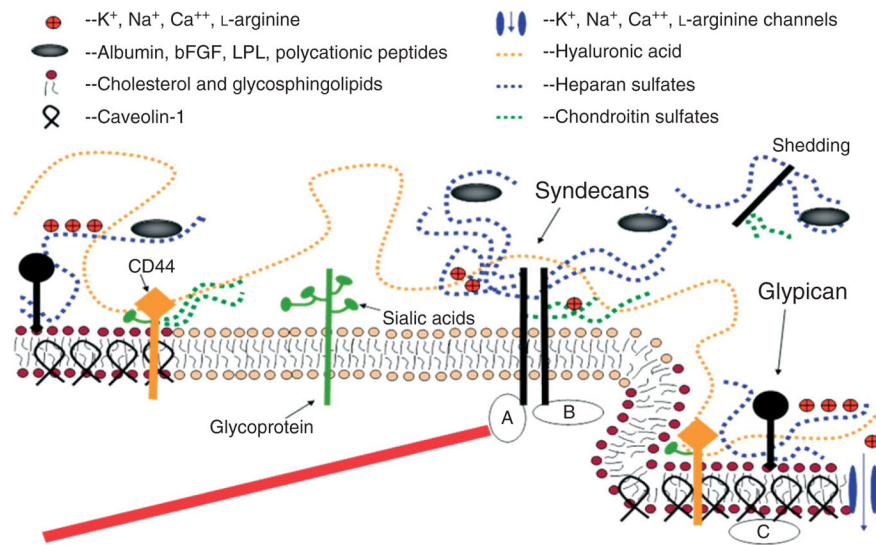
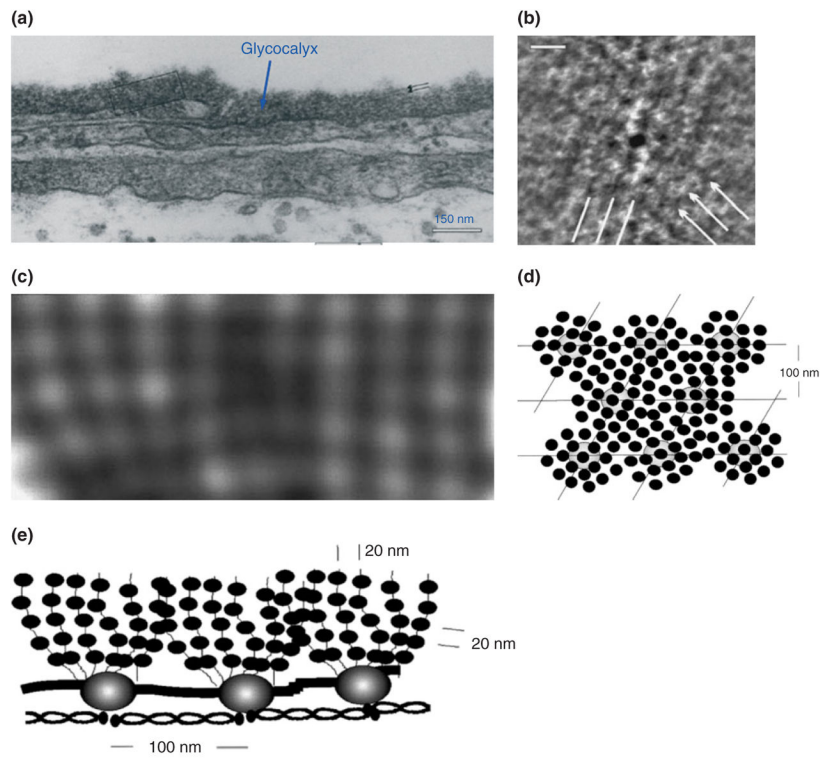


FIGURE 2.

Currently identified endothelial mechano-sensors and transducers. At endothelial cell (EC) surface: surface glycoalyx, adherences junction protein VE-cadherin, cell adhesion molecule PECAM-1, ion channels, tyrosine kinase (TK) receptor, G-protein-coupled receptors (GPCR), caveolae, primary cilia, integrins (forming FA, focal adhesion, with ECM protein). In EC cytoskeleton: microtubules and actin filaments. Nesprins connect EC cytoskeleton to nucleus. (Reprinted with permission from Ref 6. Copright 2011 The Japanese Pharmacological Society)

**FIGURE 3.**

A conceptual and simplified view for proteoglycans and glycosaminoglycans (GAGs) of the endothelial surface glycocalyx (ESG). Caveolin-1 associates with regions high in cholesterol and sphingolipids in the EC membrane (darker circles, left), and forms cave-like structures, caveolae (right). Glypicans, along with their HS chains (blue dotted lines) localize in these regions. Transmembrane syndecans are shown to cluster in the outer edge of caveolae. Besides HS, syndecans also contain CS, lower down the core protein (green dotted lines). A glycoprotein with its short oligosaccharide branched chains and their associated SA ‘caps’ are displayed in the middle part of the figure (green). HA is a very long GAG (orange dotted line), which weaves into the glycocalyx and binds with CD44. Transmembrane CD44 can have CS, HS and oligosaccharides attached to it, and localizes in caveolae. Plasma proteins (gray), along with cations and cationic amino acids (red circles) are known to associate with GAGs. (a) The cytoplasmic domains of syndecans can associate with linker molecules which connect them to cytoskeletal elements (red line). (b) Oligomerization of syndecans helps them make direct associations with intracellular signaling effectors. (c) A series of molecules involved in eNOS signaling localize in caveolae. (Reprinted with permission from Ref 18. Copyright 2006 Blackwell Publishing Ltd)

**FIGURE 4.**

EM images and structural model for the endothelial surface glycocalyx (ESG). (a) Electron micrograph of a plastic section of a frog mesenteric capillary. (Reprinted with permission from Ref 47). The thickness of glycocalyx is ~100 nm. (b) Enlarged part of the glycocalyx shown in (a) after processed by autocorrelation functions (ACFs). It shows a quasi-hexagonal arrangement of spacing 80–120 nm. (c) Larger view of glycocalyx showing more detailed structures. (d) En face view (from the luminal side) of a structural model for the glycocalyx corresponding to the EM image shown in (b). (e) Side view of the model for the glycocalyx corresponding to the EM image shown in (c) (Reprinted with permission from Ref 43. Copyright 2001 Elsevier Science)

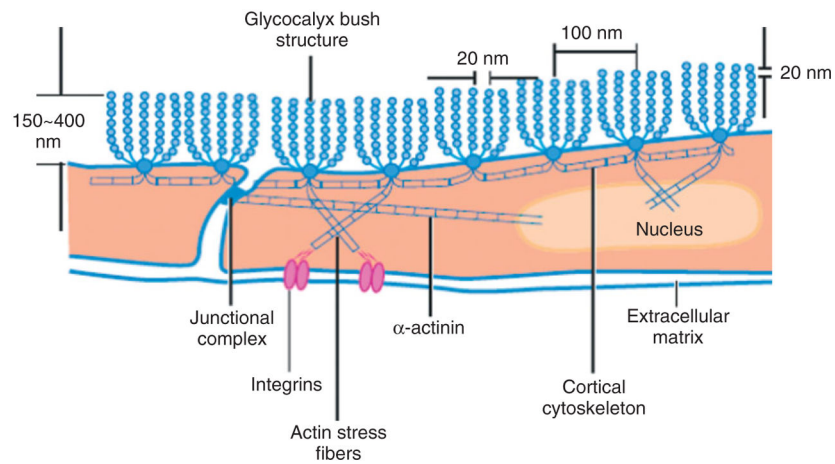


FIGURE 5.

Sketch of a conceptual model for the arrangement of core proteins in the ESG and its anchorage to the underlying actin cortical cytoskeleton. This model is based on the EM observation as shown in Figure 4. (Reprinted with permission from Ref 44. Copyright 2007 Annual Reviews)